

THE CENTRAL REGION OF THE U400 CYCLOTRON. THE CALCULATION OF THE ACCELERATING BEAM DYNAMICS FOR THE FIRST ORBITS AFTER THE INJECTION.

I.A. Ivanenko

FLNR JINR, Dubna, 141980, Russia

The results of calculations of the accelerating beam dynamics in the central region of the U-400 cyclotron are presented. The calculations have been done for several configurations of the accelerating structure with an axial injection system and an ECR ion source. The calculations showed that the optimal location of the elements of the accelerating structure can allow the intensity of ion beams with $A/Z = 5 \div 10$ to be increased by a factor of $2 \div 1.5$.

1. INTRODUCTION

The performance of the cyclotron central region is essentially determined by first few turns of the accelerated ion beams. Usually, the variation of the isochronous cyclotron magnetic field influences on the vertical focusing of the accelerated ions beginning with the 3÷5 turns. For the 1÷3 turns the vertical focusing is provided through the action of the accelerating electric field and the small magnetic field bump at the centre [1]. The most important factor of the beam radial and vertical focusing at the first turn is the correct propagation of the electric field at the ion-optic system of the accelerating gaps.

From 1978 to 1996 an internal PIG ion source was used at the U400 cyclotron. The axial injection system for the U400 cyclotron has been constructed and put into operation since the second half of 1996. In the axial injection system the ECR ion source is used. The new conditions for the ion accelerating led to the necessity for the analysis of the beam dynamics at the first turns. The beam dynamics was calculated with the CENTR program [2], based on the Lorentz equations.

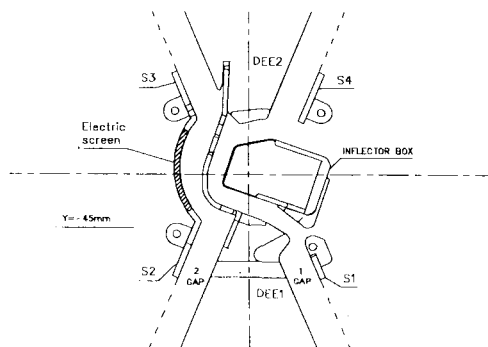


Fig. 1 The U400 cyclotron centre.

The electric field distribution is represented:

- for the first turn by the 3-dimensional electric potential distribution, calculated by means of the program code RELAX3D [3].
- for the next turns by an analytical expression [2,4].

The magnetic field distribution was taken from the data on the cyclotron magnetic field measurements.

The geometrical description of the U400 cyclotron accelerating structure was taken as the limitation on the beam dynamics calculations. This description was based upon the RELAX3D input file. To calculate the cyclotron radial acceptance, the limitations of the energy dispersion and the turn centre positions has been used.

2. THE INJECTED BEAM EMITTANCE

The efficiency of the ion beam acceleration in the cyclotron in essential extent is determined by the emittance of the injected beam. The calculations of the beam radial and vertical emittances after the spiral inflector were done by means of the program code CASINO [5,8]. The angular position of the inflector relative to the cyclotron accelerating system can be changed. It gives us the possibility to adjust the beam injection system. The changing in the inflector angular position result in the positions of the radial and vertical emittances being changed. The results of the calculations of the beam radial and vertical emittances for some inflector angular positions are presented in figures 2 and 3.

In these figures: R is the average radius of the beam position;

ΔG - the angle between the beam velocity direction and the perpendicular to the beam position's radius-vector.

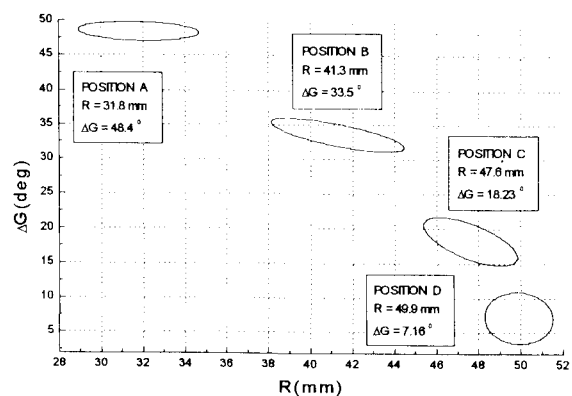


Fig. 2 The radial emittances for some angular positions of the inflector.

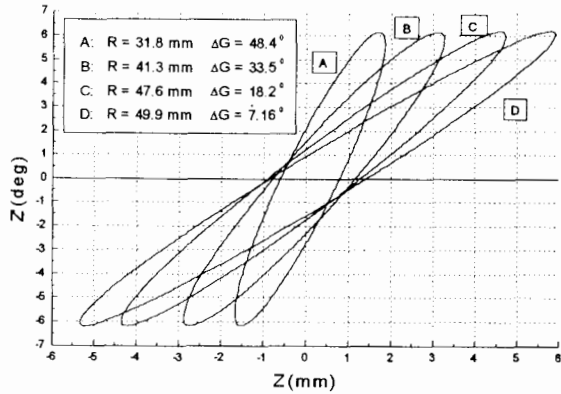


Fig. 3 The vertical emittances for some angular positions of the inflector.

3. THE BEAM DYNAMICS FOR THE INITIAL GEOMETRY OF THE CYCLOTRON CENTRE

The calculations of the beam dynamics for the initial geometry of the cyclotron centre showed the predominance of the beam vertical defocusing at the second accelerating gap. The vertical trajectories of the accelerated ion with $A/Z=10$ and the distribution of the vertical component of the electric field E_z (at the same time) along the ion angular position are presented in figure 4. The initial phase of the given ion is $\varphi_0 = -60^\circ$. The start vertical positions of the ion: $Z_0 = 2\text{mm}$ and $Z_0' = 3^\circ, 5^\circ, 7^\circ$.

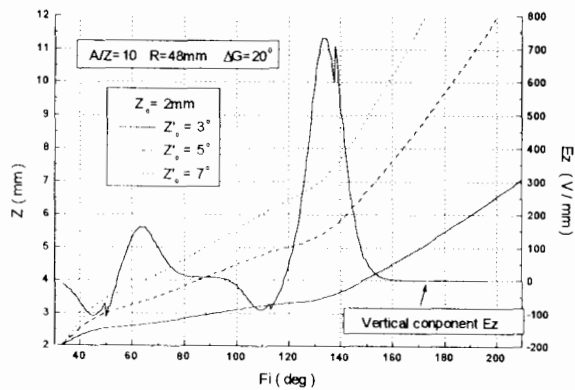


Fig. 4 The vertical trajectory of the accelerated ion with $A/Z=10$ and the distribution of the vertical component of the electric field E_z along the ion position angle

According to figure 4 the vertical motion of the accelerated beam is defocalized at the ion-optic lens of the second accelerating gap (the azimuth angle Φ from 100° to 150°). The 3-dimensional electric potential distribution, calculated by means of the program code RELAX3D, showed two problems with the second accelerating gap geometry. On the one hand, the puller stem of the first dee limits the electric field penetration into the dee system. The influence of the ion-optic lens focusing part on the accelerated ion vertical motion is decreased. On the other

hand, the electric screen between the S2 and S3 dummy dees, see figure 1, is cut off before the S2 dummy dee. The influence of the ion-optic lens defocusing part on the accelerated ion vertical motion is increased. The vertical distribution of the electric potential along the $Y=-45\text{mm}$ line, see figure 1, for the initial geometry of the centre is presented in figure 5. This distribution shows the predominance of the ion-optic lens vertical defocusing part in the second accelerating gap.

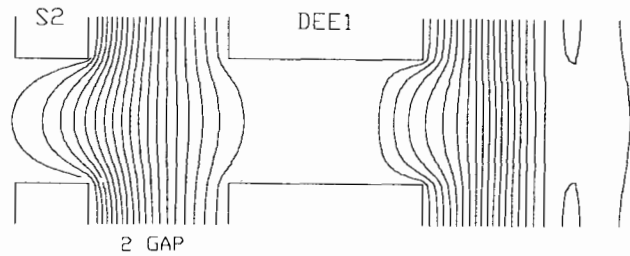


Fig. 5 The vertical distribution of the electric potential along the $Y=-45\text{mm}$ line for the initial geometry of the cyclotron centre.

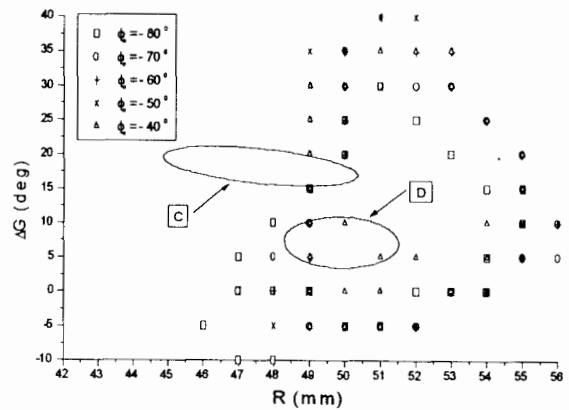


Fig. 6 The cyclotron radial acceptance and the injected beam radial emittance ($A/Z=10$) for the initial geometry of the cyclotron centre.

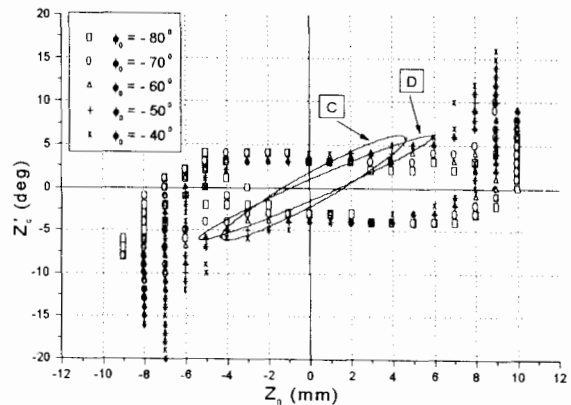


Fig. 7 The cyclotron vertical acceptance and the injected beam vertical emittance ($A/Z=10$) for the initial geometry of the cyclotron centre.

The positions of the radial and vertical cyclotron acceptances and the injected beam emittances are presented in figures 6 and 7. The ion beam with $A/Z=10$ was taken into account. According to figures 2 and 3, the “C” and “D” positions of the inflector were taken.

In the present calculations the following limits were taken:

- The first five turns were taken into account;
- The position of the calculated turns relative to the cyclotron centre $R \leq 15\text{mm}$;
- The energy dispersion is $\Delta E/E \leq 15\%$.

The efficiency of the injected beam acceleration depends on the position of the beam radial and vertical emittances regarding the cyclotron acceptances. The not matching of the beam emittances with the cyclotron acceptances leads to the beam losses, see figures 6 and 7. The calculations of the beam dynamics of the ions with $A/Z=5$ showed the beam losses at the inner pillar of the first dee stem and at the electric screen between the S2 and S3 dummy dees. Besides, the trajectories of the ion with $A/Z=5$ for the start positions matched to the “C” and “D” radial emittance positions are shown in figure 8.

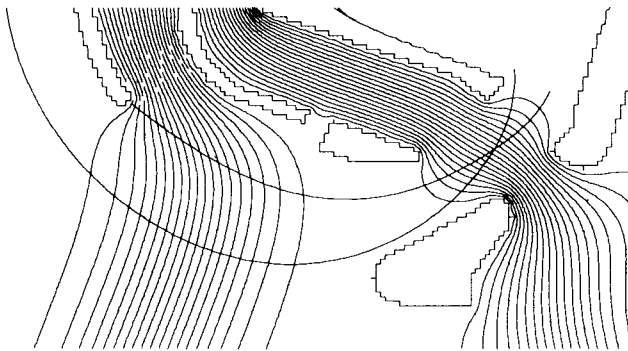


Fig.8 The trajectories of the ion with $A/Z=5$ for the start positions $R=41\text{mm}$, $\Delta G=35^\circ$; $R=50\text{mm}$, $\Delta G=7^\circ$ (“C” and “D” radial emittance positions, figure 2).

The presented results show the necessity for the correction of the cyclotron centre ion-optic system.

4. THE CORRECTION OF THE CYCLOTRON CENTRE ION-OPTIC SYSTEM

According to figures 2 and 3, a change in the inflector angular position exerts the most effective influence on the radial beam injection. Then the problem of the correction of the cyclotron centre ion-optic system comes to suppressing the beam vertical defocusing at the first and second accelerating gaps. The calculations of the beam dynamics were done for some models of the first and second accelerating gaps structures. The suppression of the beam vertical defocusing in the simulated case is presented in figure 9. The beam vertical emittance is matched to the cyclotron acceptance. The simulation consists in neglect the

influence of the first gap vertical defocusing part on the ion motion. For the real case the beam vertical defocusing can be suppressed by changing the position of the electric screen relative to the second gap as well as the position of the pillars of the first dee stem. Besides, the electric field penetration into the S2 dummy dee system would be restricted by pillar installation. Unfortunately, the pillar can not be effectively placed because of its conflict with the ion trajectory positions ($A/Z=5 \div 10$).

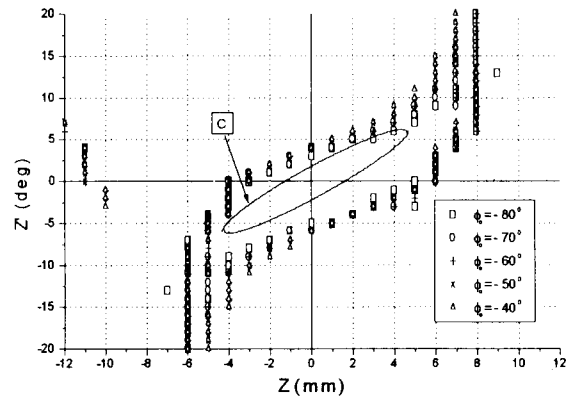


Fig. 9 The beam vertical emittance ($A/Z=10$) and cyclotron acceptance for the ideal case of the suppression of the beam vertical defocusing.

The penetration of the electric field into the S2 dummy dee system can be restricted by lengthening the electric screen up to the second gap forming line, see figures 1 and 12. Then the vertical defocusing is reduced. The positions of the cyclotron radial and vertical acceptances and the injected beam emittances ($A/Z=10$) are presented in figures 10 and 11. According to figure 10, the effective radii of the cyclotron radial acceptance position are shifted to the cyclotron centre. As a result, the position of the electric screen will be not so critical to accelerate the ions with $A/Z=5$, see figure 8.

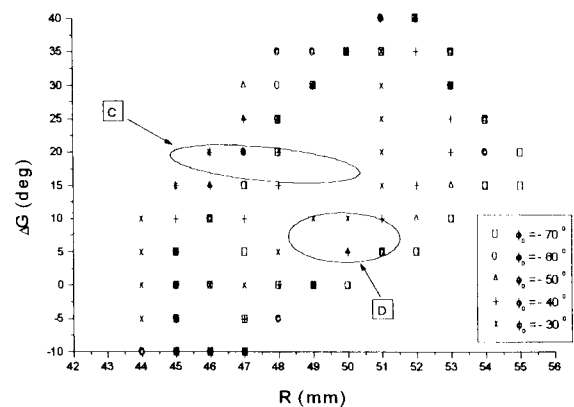


Fig. 10 The cyclotron radial acceptance and the injected beam radial emittance ($A/Z=10$) for the geometry of the cyclotron centre after correction.

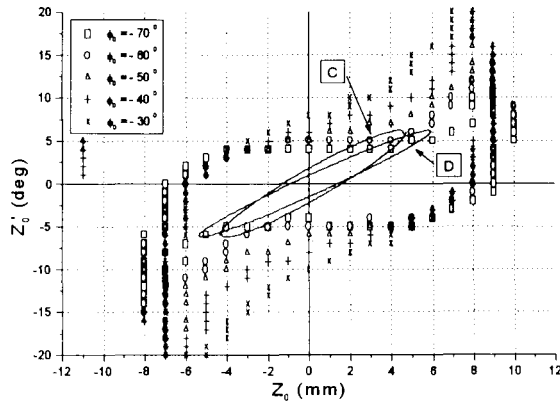


Fig. 11 The cyclotron vertical acceptance and the injected beam vertical emittance ($A/Z=10$) for the geometry of the cyclotron centre after correction.

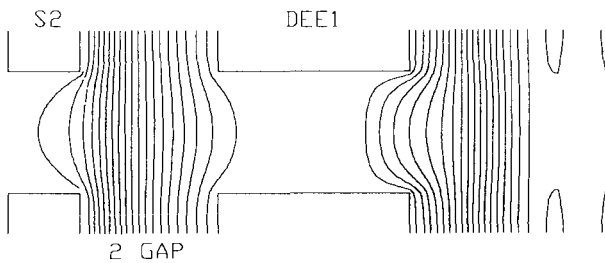


Fig. 12 The vertical distribution of the electric potential along the $Y=-45\text{mm}$ line for the geometry of the cyclotron centre after correction.

5. THE ACCELERATING COEFFICIENT

The accelerating coefficients K_r and K_z are presented as a ratio of the acceptance and emittance intersection squares to the emittance square. The total coefficient K is presented as [6,7]:

$$K = \frac{\int (K_r * K_z) \delta \varphi_0}{\Delta \varphi_0}, \quad (1)$$

where: φ_0 is the initial phase of the accelerated ion relative to the electric field phase;
 $\Delta\varphi_0$ is the range of the initial phases.

In the present paper $\Delta\varphi_0 = 360^\circ$ (the period of the electric field frequency) was taken. The vacuum condition and the vertical gradients of the magnetic field were not taken into account. The accelerating coefficients of the ion beam with $A/Z=10$ for the initial geometry of the cyclotron centre and after the correction are presented in the table 1. These coefficients have been calculated for the “C” and “D” emittances positions, see figures 2 and 3. According to table 1, the best angular position of the inflector for the initial geometry of the centre is the “D” position. After correction of the cyclotron centre geometry, the accelerating coefficient value can be expected to increase by a

factor of 1.5. The same calculations for the ion beam with $A/Z=5$ showed the expected increase in the accelerating coefficient value by a factor of 2.

Table 1: The accelerating coefficients for the ion beam with $A/Z=10$. The initial geometry of the cyclotron centre and geometry after correction.

	“C”	“D”
Initial geometry	4%	11%
After correction	16%	9%

6. CONCLUSION

A Change in the inflector angular position exerts the most effective influence on the radial beam injection. At the same time, a change in the vertical beam injection efficiency is not very significant. The calculations of the beam dynamics for the initial geometry of the cyclotron centre have shown the predominance of the beam vertical defocusing at the second accelerating gap. The non optimal location of the elements of the second accelerating gap leads to the asymmetric distribution of the electric field vertical component. A simulation of the electric screen positions between the S2 and S3 dummy dees and the first dee stem pillar have been carried out. This simulation has shown that the optimal location of the elements of the accelerating structure can allow the intensity of the ion beams with $A/Z = 5 \div 10$ to be increased by a factor of $2 \div 1.5$, respectively.

REFERENCES

- [1] 12 International Conference On Cyclotrons And Their Applications, Germany, 1989, ISBN 981-02-0086-2, p. 327.
- [2] I. Ivanenko, JINR Preprint, P9-96-409, Dubna, 1996
- [3] Relax3D User’s Guide and Reference Manual, TRI-CD-88-01.
- [4] J. Sura INR 1964/XXV/PL/A, Swierk, 1983.
- [5] CASINO User’s Guide and Reference Manual, TRI-N-89-19
- [6] G. Gulbekian, I. Ivanenko, Scientific Report 1995-1996, FLNR, JINR, Dubna, p. 284, E7-97-206.
- [7] I. Ivanenko, 5/98 In. Rep., Warsaw University, 1998
- [8] Y. Oganessian et al., Scientific Report 1995-1996, FLNR, JINR, Dubna, p. 275, E7-97-206.